AIAA JOURNAL
Vol. 41, No. 12, December 2003

Effects of Pulsing on a Vortex Generator Jet

H. Johari* and G. S. Rixon†
Worcester Polytechnic Institute, Worcester, Massachusetts 01609

The evolution of a pulsed vortex generator jet embedded in a turbulent boundary layer was examined experimentally. The jet, which was pitched 45 deg and skewed 90 deg, had a velocity three times greater than the freestream. The velocity field in planes normal to the freestream was measured by the particle-image-velocimetry method at four stations downstream of the jet exit. The pulsed jet created a starting vortex ring followed by a pair of counter-rotating streamwise vortices, one of them being markedly stronger. Phase-averaged data indicate that the maximum circulation and peak vorticity of the stronger vortex are approximately 30% greater than the average values for a steady jet with the same velocity. However, circulation averaged over the entire pulse was less than that for a steady jet at the same location. The core of the primary streamwise vortex penetrates approximately 50% farther into the boundary layer than a steady jet with the same velocity. The larger penetration takes place during the initial portion of the pulse and is caused by the jet starting vortex ring.

Introduction

THE effects of pulsing on the structure and development of a vortex generator jet (VGJ) are investigated. Specifically, the evolution of these vortices in a flat plate turbulent boundary layer was quantified. Pulsed jets were considered because several past investigations by McManus et al.[1–3] have shown that pulsing can significantly improve the performance of VGJs used for separation control. With the same average mass-flow rate, a pulsed jet delayed flow separation and stall on an airfoil to a higher angle of attack in comparison to a steady VGJ.[2] Moreover, a significantly larger area on the airfoil surface was affected by the pulsed jet. Pulsed VGJs have also shown great promise in reducing separated regions on low-pressure turbine blades[4] and aircraft configurations.[5] Even though the pulsed VGJ performance is superior to the steady VGJ, the mechanisms responsible are not well understood. The present study was undertaken to gain a better understanding of the structure of the vorticity field created by a pulsed VGJ in a turbulent boundary layer.

A schematic of a single, pulsed VGJ and the coordinate system used is shown in Fig. 1. Besides the jet-to-freestream velocity ratio $VR = V_j/U_\infty$, the ratio of jet diameter to the local undisturbed boundary-layer thickness D/δ and the jet orientation (pitch and skew angles), which are important in steady VGJ design, the pulsing frequency f, and duty cycle Δ have to be considered in pulsed jets. In the present study the jet flow was fully modulated, that is, the flow was terminated during a portion of the cycle. The duty cycle is the ratio of the jet injection time to the period of the pulse and is confined between 0 and 1; these limits refer to no flow and steady injection, respectively.

The primary effect of pulsing on the structure of freejets is the formation of a starting vortex ring during each cycle.[6,7] Pulsed freejets have shown improved entrainment in both the near and far field.[7,8] Effects of pulsing have also been investigated in transverse jets, where the jet is issued perpendicular to a crossflow and the boundary-layer interactions are minimal.[9,10] Penetration of the pulsed transverse jets into the uniform crossflow is significantly greater than that of the steady jets because of the presence of starting vortex rings at the onset of each pulse. In a flow-visualization study of pulsed VGJs,[11] the streamwise vortices likewise penetrated much deeper into the overlaying turbulent boundary layer in comparison with an analogous steady jet.

The current study investigated the characteristics of a single, pulsed vortex generator jet embedded in a flat-plate turbulent boundary layer by the particle-image-velocimetry (PIV) technique for acquiring instantaneous planar velocity data sets. The streamwise vorticity field resulting from pulsed jets has not been measured in the past studies. Phase averaging was utilized to examine the evolution of the jet-generated vortices and their position within the turbulent boundary layer. The data were used to address the following questions:

1) How do the circulation, peak vorticity, and position of the primary streamwise vortex generated by a pulsed VGJ compare with a steady jet having the same velocity ratio? How do these parameters change with distance from the jet source?

2) How do the peak vorticity, position, and circulation vary during the cycle?

3) What role does the starting vortex ring play in the resulting primary streamwise vortex?

The experimental setup is described in the next section. The scaling of pulsed jets (based on the current observations) is discussed following the Results section.

Throughout this paper jet-to-freestream velocity ratio has been considered as the main parameter representing the jet strength. However, other parameters such as the jet momentum flux or vorticity flux can also be adopted. Although vorticity flux is perhaps a more fundamental measure, it is much more difficult to quantify in different setups, especially in practical systems. Momentum flux ratio would be equivalent to VR for incompressible, isothermal flows with similar jet exit areas (the present case). Hence, the choice of VR as the characterizing parameter in pulsed VGJ applications appears to be valid.

Experimental Setup

The experiments were conducted in a free-surface recirculating water tunnel at a freestream velocity of 20.3 cm/s. The freestream turbulence intensity in the test section was measured with a laser-Doppler-velocimetry (LDV) system to be 1.5% at this velocity. A schematic of the test section and the setup is shown in Fig. 2.

The boundary layer developed on a clear acrylic flat plate submerged approximately 0.1 m below the free surface. The plate spanned the width of the test section and measured 1.40 m in length. The leading edge of the plate was elliptical, and the boundary layer was tripped by a staggered set of 60-grit sandpaper strips, placed at 2.5 and 5 cm downstream of the leading edge. The boundary-layer profile at the VGJ location (1.15 m from the leading edge) was measured by the LDV system. The turbulent boundary layer was two

Presented as Paper 2002-2834 at the AIAA 1st Flow Control Conference, St. Louis, MO, 24–26 June 2002; received 17 July 2002; revision received 16 June 2003; accepted for publication 2 July 2003.

*Professor, Mechanical Engineering Department. Associate Fellow AIAA.

†Research Associate; currently Aerospace Engineer, Arnold Engineering Development Center, Arnold Air Force Base, TN 37389. Member AIAA.

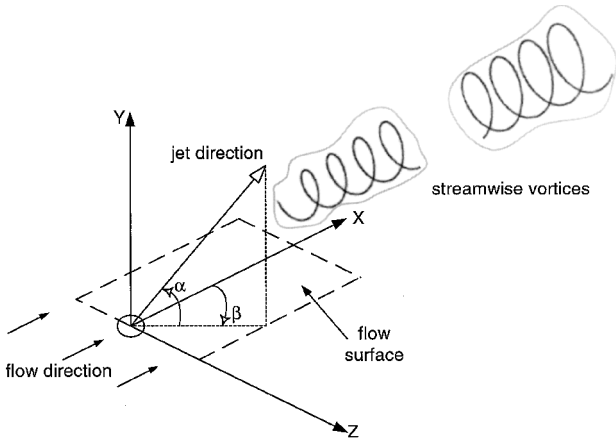

Fig. 1 Schematic of a pulsed vortex generator jet and associated coordinate system. The pitch angle is α, and the skew angle is β.

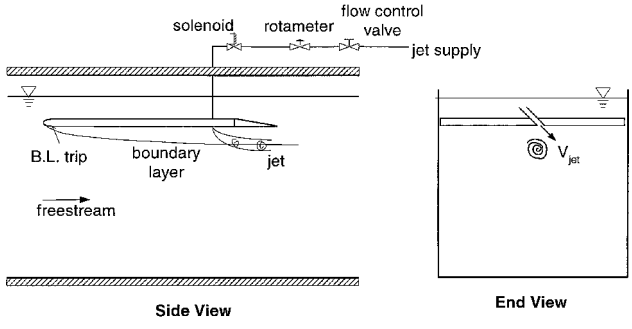

Fig. 2 Schematic of the water-tunnel test section and the experimental setup.

dimensional with a thickness of $\delta \approx 3.4$ cm. There was a distinct logarithmic region spanning from $y^+ \approx 30$ to 160; the best-fit line to the data in this range had a slope of 1/0.41. The displacement and momentum thickness were measured to be 4.3 and 3.3 mm, respectively, resulting in a shape factor of 1.3.

A single jet was mounted flush in the flat plate 1.15 m downstream of the leading edge using a 5-cm-diam plug. The jet diameter D was 4.76 mm, and its orientation was fixed at a 45-deg pitch angle and a 90-deg skew angle. Previous work has shown this orientation to be an optimal configuration for producing a strong streamwise vortex.[12] The ratio of jet diameter to the boundary-layer thickness D/δ at the jet exit was 0.14. The location of the jet was chosen to allow for a fully developed turbulent boundary layer with sufficient thickness for high spatial resolution velocity measurements. Smaller values of δ would result in reduced spatial resolution, whereas larger δ values would further decrease the D/δ parameter.

A pressurized diaphragm tank supplied the jet, and the flow was controlled using a precision needle valve. A small solenoid valve was placed after the rotameter to allow for the modulation of the jet flow rate. A power supply coupled with a function generator supplied a square wave to the valve. To focus on the effects of pulsing, a single jet velocity V_j of 0.6 m/s was chosen. This average jet velocity results in a velocity ratio $VR = 3$. The mean jet velocity was quantified through volume flow measurements of 100 pulses.

A single pulsing frequency of 1 Hz was selected in our experiments based on a previous flow-visualization study.[11] In that study, which utilized the same setup, the 1-Hz frequency resulted in the largest contrast between the penetration of the steady and pulsed jets. Using the jet diameter and velocity, the 1-Hz pulsing frequency reduces to a forcing Strouhal number of $fD/V_j = 0.008$. This is significantly smaller than the Strouhal frequency of 0.3 used for forcing of free jets. The pulsing frequency reduced by the freestream velocity and δ becomes $f\delta/U_\infty = 0.17$.

The duty cycle Δ, defined as the ratio of jet injection time to pulse period, was varied independent of the pulsing frequency. The jet injection time τ was then given by Δ/f. Two duty cycles of 0.5 and 0.25 were chosen in the experiments to investigate the effects of Δ. Operation at duty cycles smaller than 0.25 resulted in inadequate pulses because of the finite response time of the solenoid valve and the fluid delivery system. Moreover, at a frequency of 1 Hz, the jet pulse duration is only 0.25 s. Because the sampling rate of our PIV system is 15 Hz, only four data fields could be measured during the pulse. Therefore, neither duty cycles smaller than 0.25 at $f = 1$ Hz nor higher frequencies at $\Delta = 0.5$ were attempted.

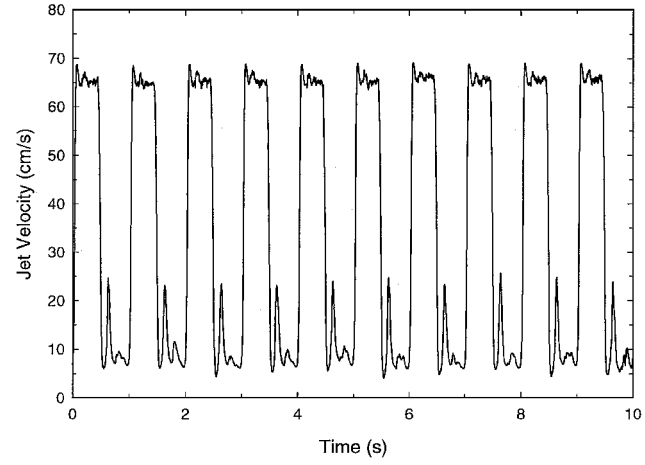

Fig. 3 Temporal variation of the jet exit velocity: $\Delta = 0.5$.

The jet-exit velocity was measured with a hot-film probe to assess the repeatability of the pulses. Time traces of the jet-exit velocity are shown in Fig. 3 for the 0.5 duty cycle. Both duty cycles reveal repeatable pulses with small (~5%) overshoots at the start of each pulse. Though there is a secondary pulse following each pulse, the volume and impulse contained therein are negligible compared to the primary pulse. Moreover, flow visualization close to the jet exit did not reveal any secondary ejection after the primary pulse. The full modulation of the jet flow is not apparent from these time traces as the hot film reads a minimum velocity even in a quiescent environment. The average length of the fluid slug ejected at the jet exit during the pulse was calculated to be 63 and 29 D for the 0.5 and 0.25 duty cycles, respectively.

The velocity measurements were carried out by the PIV technique. In these measurements the entire water tunnel, as well as the jet, was seeded with neutrally buoyant silver-coated glass spheres with an average diameter of 46 μm. The flow was illuminated by a sheet of laser light with a thickness of approximately 3 mm. The light source was a pair of pulsed Nd:YAG lasers, each of which fired independently at a frequency of 15 Hz. For all of the experiments, the laser pulse separation was set at 5 ms. The laser sheet was placed normal to the freestream so that the secondary velocity components could be measured. The laser sheet was positioned at four stations 5, 10, 20, and 30 D downstream of the jet exit. These locations correspond to data fields taken at 0.7, 1.4, 2.8, and 4.2 δ.

The cross-correlation technique was used to process the PIV images. A 30-Hz progressive scan charge-coupled device (CCD) camera with a spatial resolution of 768×480 pixels was employed. Because a pair of successive images is used for extracting the particle displacements, the resulting velocity field was sampled at 15 Hz. The image pairs were processed with a window size of 32×32 pixels and a roaming window size of 16×16 (50% window overlap). Allowing for the laser-sheet thickness of 3 mm results in an effective spatial resolution of ≈ 4 mm. Because particles moving at the freestream velocity traveled only 1 mm during the time between the pulses (5 ms), the majority of the particles remained within the 3-mm light sheet.

At each measurement station 500 instantaneous velocity fields were acquired. The streamwise vorticity field was computed from each velocity field. The primary parameters of interest were the peak vorticity in the vortex core and its location within the boundary layer, as well as the vortex circulation. Circulation was computed by integrating the velocity along a specific isovorticity contour.

The freestream velocity U_∞ and boundary-layer thickness δ were used for normalizing the measured parameters. The uncertainty in the boundary-layer thickness and freestream velocity were 1.5 and 0.5%, respectively. The jet velocity had an uncertainty value of 1%, resulting in an uncertainty of 2.5% for the velocity ratio. The placement of the laser sheet (in the axial direction) had an uncertainty of 1 mm corresponding to uncertainties of 4.2, 2.1, 1.1, and 0.7% for the four stations at $x/\delta = 0.7$, 1.4, 2.8, and 4.2, respectively. Based on the subpixel accuracy of the cross-correlation peak and the particle displacements, the measured velocities and computed vorticities are estimated to be accurate to ± 1.5 and $\pm 4.5\%$, respectively.

Because of the stretching of the fluid pulse as it moved away from the jet source, the PIV data could not be directly phase locked with the source frequency. Phase averaging of the 0.5 duty cycle was carried out by examining individual pulses and assigning phase angles to each recorded data field. This is further explained in the next section. The data for the 0.25 duty-cycle case were not phase-averaged because only four data fields were measured for each pulse. In this case the largest peak vorticity and the average of the peak vorticities during each pulse are reported. The average of peak vorticities, denoted by pulse average, was obtained by averaging the peak vorticities measured in each data field during the passage of the pulse.

Results

Flow Visualization

A side view (x–y plane) image of a pulsed jet marked with passive dye (food coloring) is shown in Fig. 4. The extent of the image is 50 D, and the duty cycle was 0.5. The starting vortex ring of the jet pulse, shown in the close-up image, is clearly discernable here. Even at such close proximity to the jet source, the starting vortex ring appears to have been influenced by the crossflow. The ring is turned in the flow direction within about one jet diameter. The vortex ring gets bent and stretched as a result of its interaction with the boundary layer, as in the jet fluid packet visible in Fig. 4 further downstream of the source. The two nearly separated portions of the elongated jet pulse in the image are noteworthy. This feature was observed for both duty cycles and for all pulses. The head of the fluid packet is the remnant of the starting vortex ring, whereas the rest is the portion of the jet following the starting ring. The two separate segments also tend to produce two peaks in the maximum vorticity within a pulse, at least near the jet source.

End-view (y–z plane) images of the jet marked with a fluorescent dye and illuminated with a laser sheet at $x = 12\ D$ (1.7 δ) are shown in Fig. 5. Three consecutive instantaneous (33 ms apart) images of the jet cross section are shown. The primary vortex rotating in the clockwise (CW) direction is clearly visible in these images. The third image corresponds approximately with the maximum streamwise vorticity during the pulse. Comparison of these images with those of a steady jet at the same axial location reveals that the primary vortex in the pulsed case is more compact and better organized. This is also confirmed by the higher maximum vorticity within the pulses.

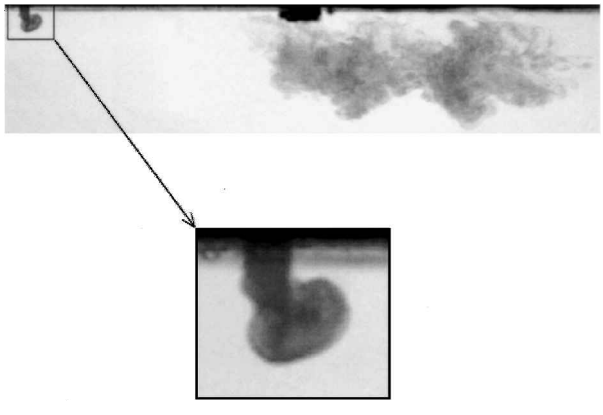

Fig. 4 Side view (x–y plane) of a pulsed jet with $\Delta = 0.5$. The extent of the image is 50 D, corresponding to 7 δ. The close-up shows the starting vortex ring of the pulsed jet. Flow is from left to right.

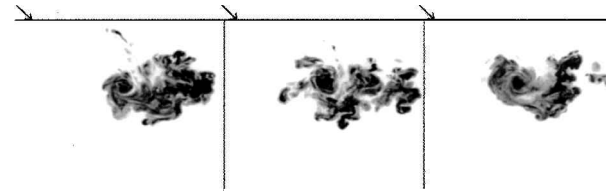

Fig. 5 Instantaneous laser-induced fluorescence images of a VGJ in the y–z plane at $x = 12\ D$ (1.7 δ). The jet was pulsed with a duty cycle $\Delta = 0.5$.

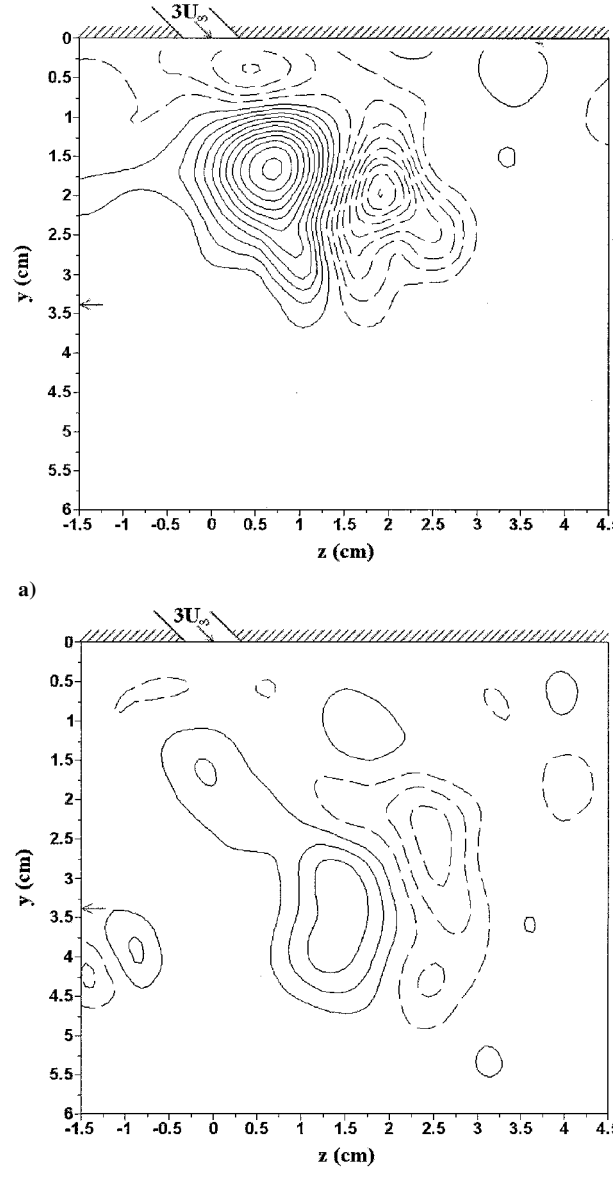

Fig. 6 Instantaneous vorticity fields for a pulsed jet at a duty cycle $\Delta = 0.25$, minimum $|\omega|$ contour is 2 s^{-1} with an increment of 2 s^{-1}: a) $x/\delta = 0.7$, and b) $x/\delta = 4.2$. Vorticity in the CW direction is indicated by solid contour lines. Arrows on the y axes indicate the approximate location of the undisturbed boundary-layer edge.

Vorticity Fields

Instantaneous vorticity fields of the pulsed jet at the first ($x = 0.7\ \delta$) and last ($x = 4.2\ \delta$) measurement stations at times corresponding to the maximum observed streamwise vorticity are shown in Fig. 6 for the 0.25 duty cycle. In both stations the primary CW vortex and the weaker counterclockwise (CCW) vortex are clearly distinguishable. The vorticity contours at the first measurement station indicate well-organized vortices with cores that have penetrated approximately halfway through the boundary layer. Although the

CCW vortex is weaker in terms of circulation and peak vorticity, its core position within the boundary layer is comparable to its stronger CW counterpart. The vorticity contours and the peak vorticity for the 0.5 duty cycle are quite similar to the 0.25 duty cycle shown in Fig. 6.

As the pulse moves downstream to $x = 4.2\ \delta$, the primary CW vortex and its CCW counterpart weaken and become less organized. The smaller duty-cycle case has a more rapid decay than the 0.5 duty-cycle jet. The vortex cores for both duty cycles move further away from the wall and the jet source. The background vorticity that had levels generally below 4 s^{-1} is distinguishable by the single contour curves in the vorticity plots. The considerable CCW vorticity contours beneath the primary CW vortex at $x = 0.7\ \delta$ disappeared by the last measurement station at $x = 4.2\ \delta$.

To differentiate the coherent motions associated with the pulsed jet from the incoherent background motions, the velocity fields were phase averaged. One of the difficulties with phase averaging of the data was the loss of phase coherence as the jet pulse traveled downstream. Even at the closest measurement station at $x = 0.7\ \delta$, the duration of the pulses was approximately 10% longer than at the nozzle exit. Moreover, the pulses continued to elongate further as they convected in the streamwise direction. For this reason, at each measurement station the data field having the largest maximum vorticity within each pulse was designated to be at a phase angle of zero. Data fields prior to and following this specific field were labeled consecutively at 24-deg phase angle increments, corresponding to the 15-Hz sampling rate. In other words, the measured data fields at each station were shifted so that the fields with the largest peak vorticity values were aligned. Then, the data fields were averaged accordingly. The pulse duration was determined from the data fields in which the peak vorticity was greater than the measured background level of 4 s^{-1}.

A sequence of phase-averaged vorticity fields for the 0.5 duty cycle at the $x = 2.8\ \delta$ station is shown in Fig. 7. At this station there are nine data fields with peak vorticities above the peak background value. The first vorticity field in Fig. 7 resembles a slanted vortex pair, associated with the starting vortex ring (see Fig. 4). As

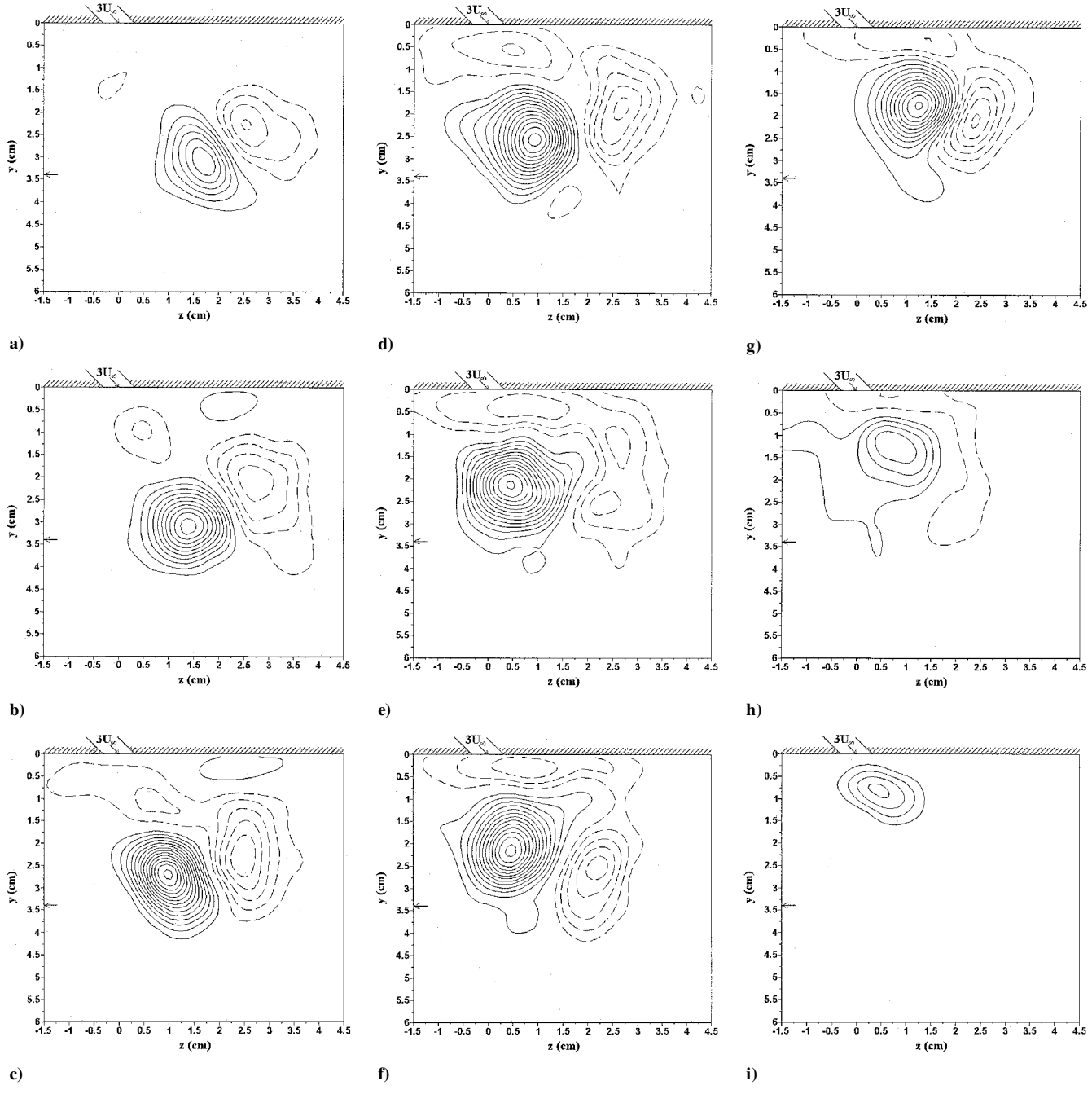

Fig. 7 Phase-averaged vorticity fields for the 0.5 duty-cycle jet at $x/\delta = 2.8$. Fields a)–i) correspond to phase angles of −96 deg to +96 deg, in increments of 24 deg. Minimum $|\omega|$ contour is 2 s^{-1} with an increment of 2 s^{-1}.

time evolves, the primary CW vortex strengthens at first, and then it weakens in the last four fields. The core position, indicated by the maximum vorticity, reaches its greatest distance from the wall in the second field. Then, the core retracts back toward the wall. The weaker CCW vortex has a similar behavior. Note that phase averaging did not wipe out the weaker CCW vortex. Also, there is CCW vorticity present between the primary CW vortex and the wall for most of the cycle.

Peak Vorticity

The peak vorticity associated with the primary vortex was extracted from the phase-averaged data and is presented in Fig. 8. The uncertainty in the normalized vorticity is approximately 7%. The field with the largest peak vorticity at the phase angle of zero corresponds approximately to the middle of the pulse. At the two stations closer to the jet source, the peak vorticity rises rapidly and reaches a maximum in the middle of the pulse. Afterward, the peak vorticity decreases rapidly. For the two farthest stations the rise and the subsequent fall of the peak vorticity is gentler. The peak vorticity appears to remain relatively constant in the middle of the pulse at these two stations. There appears to be two peaks in the phase-averaged data at the $x = 0.7\,\delta$ station, consistent with the two portions seen in Fig. 4. Farther downstream, the two peaks become indiscernible. The pulse duration, as quantified by the portion of the time that the peak CW vorticity was greater than the background level, increases with the downstream distance from the source. At the last measurement station at $x = 4.2\,\delta$, the pulse was over 30% longer than at the source.

The decay of peak vorticity for the pulsed cases is compared with the steady jet at the same velocity ratio in Fig. 9. Both the decay of the maximum within the pulse and the average over the pulse duration are considered. The steady-jet data can be represented by the expression $\omega_{max}\delta/U_\infty = 1.8VR\exp(-0.24x/\delta)$, found in our prior experiments.[13] The highest peak vorticity within the pulse is approximately 30% greater than the steady-jet value. On the other hand, the value of peak vorticity averaged over the pulse duration is less than its steady-jet counterpart for all x/δ stations considered. The peak vorticity of the pulse appears to decay exponentially with x, analogous to the steady jet. However, the decay of vorticity averaged over the pulse duration is better represented by a power law. Based on the peak vorticity characteristics, the steady jet produces a primary streamwise vortex with larger average vorticity. Pulsing does not appear to increase average vorticity of the primary vortex.

Circulation

The phase-averaged circulation of the primary CW vortex is shown in Fig. 10. The phase angle of zero corresponds to the data field with the largest peak vorticity. The circulation was computed on the isovorticity contours of 0.5 s^{-1}. The uncertainty of normalized circulation is estimated to be 4.5%. At the measurement station closest to the jet source, circulation increases rapidly after the arrival of the jet pulse. Circulation remains approximately constant and then decreases sharply. At stations farther downstream, the circulation rises and falls more slowly. Both the peak circulation within the pulse and the average circulation decrease with distance from the source. The distributions in Fig. 10 appear to evolve from a top hat to more of a rounded trace as the pulse moves downstream.

The decay of circulation with axial distance is examined in Fig. 11, where both the maximum circulation within the pulse and the average over the pulse extent are considered. The exponential decay of circulation found in steady jets[13] is also included in the plot.

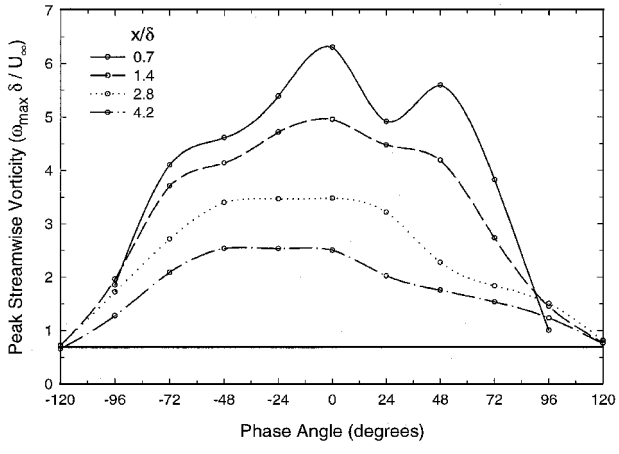

Fig. 8 Peak streamwise vorticity extracted from the phase-averaged data: ——, the background vorticity level.

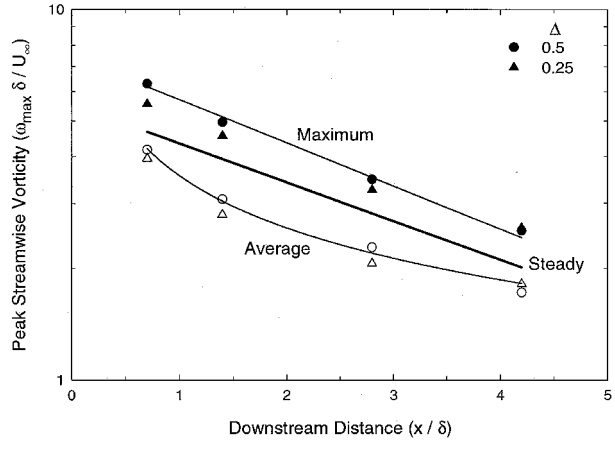

Fig. 9 Dependence of peak streamwise vorticity on downstream distance: ▲, ●, maximum values within the pulse; △, ○, values averaged over the pulse duration; ——, steady-jet behavior[13]; and the fine lines are the best-fit exponential decay to the 0.5 duty-cycle data.

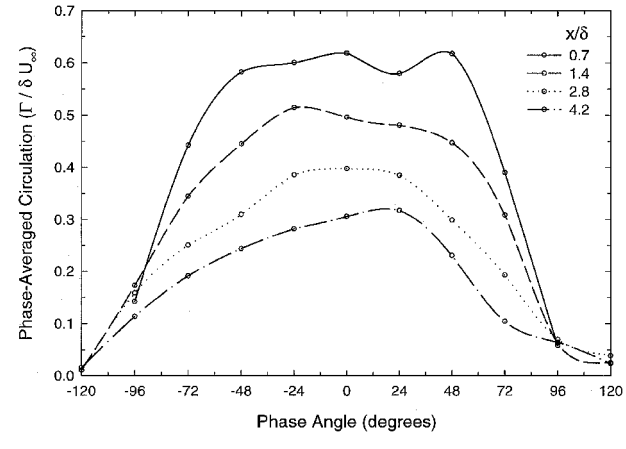

Fig. 10 Circulation measured from the phase-averaged data. Circulation was computed on 0.5 s^{-1} isovorticity contours.

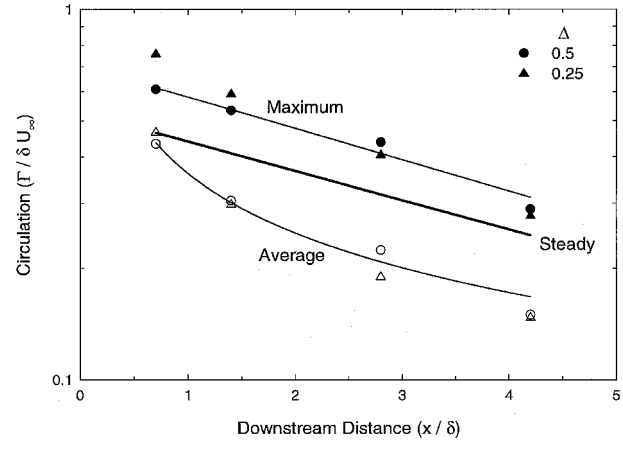

Fig. 11 Dependence of circulation on downstream distance: ▲, ●, maximum values within the pulse; △, ○, values averaged over the pulse duration; ——, steady-jet circulation[13]; and the fine lines are the best-fit exponential decay to the 0.5 duty-cycle data.

For the 0.5 duty-cycle case, the largest circulation within the pulse decays exponentially and is approximately 30% greater than that of the steady jet. The decay rate for the steady jet and the maximum circulation within the pulse are comparable for the 0.5 duty cycle. The maximum circulation of the 0.25 duty-cycle case is greater than that of $\Delta = 0.5$ close to the jet source; however, it decays faster. At the last two measurement stations the maximum circulation in the pulse is comparable for the two duty cycles.

As far as the circulation averaged over the pulse is concerned, the values for the two duty cycles are comparable and less than the steady-jet value for $x > 0.7\ \delta$. The decay of average circulation within the pulse is best characterized by a power law, and the decay rate is greater than that of the steady jet. Thus, the primary vortex produced by a steady jet has a larger average circulation than the vortices produced by pulsed jets.

Considering the evolution of VGJs in turbulent boundary layers, one can inquire about the role of boundary-layer characteristics, specifically turbulence. We believe that the primary function of boundary-layer turbulence in this problem is in terms of the loss of coherence in streamwise vortices and the associated decay of peak vorticity and circulation. The initial values of these parameters are set largely by the jet-exit parameters. Unorganized vorticity present within a turbulent boundary layer interacts and distorts/destroys the coherent vorticity produced by the jet. The decay of vortices also affects their penetration within the boundary layer.

Vortex Core Position

The wall-normal and spanwise position of the primary vortex core (y_c/δ, z_c/δ) was extracted from the phase-averaged data and is presented in Fig. 12. The uncertainty of the normalized core location is estimated to be 2.5%. The primary vortex core moves rapidly away from the wall after the arrival of the pulse, reaching a maximum value in the first portion (~20%) of the pulse. Then, the vortex moves back toward the wall and the jet source. This trend is also evident in the phase-averaged vorticity fields of Fig. 7. In the early part of the pulse, the vortex core nearly reaches a location corresponding to the undisturbed boundary-layer thickness at the last two measurement stations. In the spanwise direction the maximum displacements are approximately 0.5δ from the jet source. These large displacements are caused by the passage of the starting vortex ring, which penetrates deeper into the boundary layer. Large penetration of the starting vortex ring has also been observed in pulsed transverse jets.[9,10] The movement of the vortex core in the wall-normal and spanwise directions back toward the wall and the jet source, after the passage of the starting ring, is caused by the trailing steady jet. The nearly identical vortex core positions during the pulse passage at the last two measurement stations indicates that the VGJ vortices are fully developed by about 3δ, and the near-field vortex development is complete at this point.

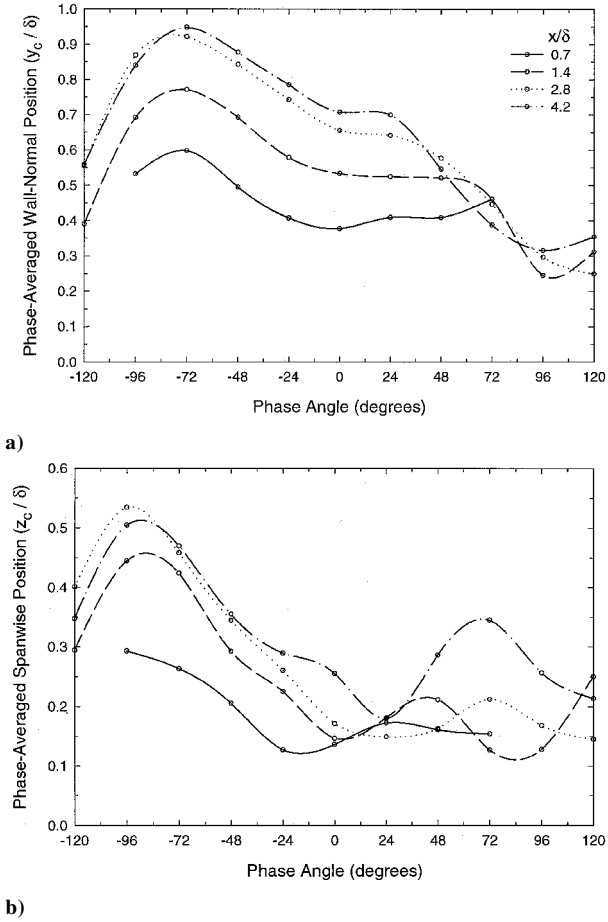

Fig. 12 Variation of phase-averaged a) wall-normal and b) spanwise position of the primary vortex core during the pulse passage.

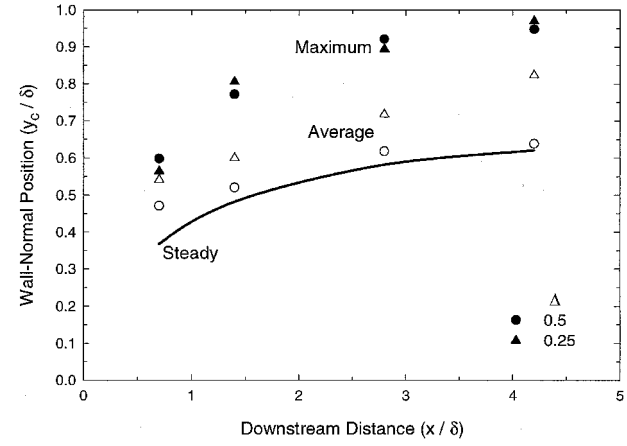

Fig. 13 Dependence of the wall-normal vortex core position on downstream distance: ▲, ●, maximum values within the pulse; △, ○, values averaged over the pulse duration; and ——, steady-jet behavior.[13]

The wall-normal position of the primary vortex core generated by the pulsed jets is compared with that of the steady jet in Fig. 13. The mean vortex core position in the steady jet is always closer to the wall than the pulse-averaged location for both duty cycles. It is especially noteworthy that the 0.25 duty-cycle case results in a larger average penetration than the $\Delta = 0.5$ case. This is because the initial peak is averaged over a shorter pulse period. As expected, the maximum penetration within the pulse is significantly greater than that of the steady jet. The maximum penetration is comparable for the two duty cycles examined because the starting ring for both cases should have similar characteristics. Based on the vortex core placement within the boundary layer, the pulsed jet has a significant advantage over the steady jet.

Scaling

Based on the preceding findings, the major advantage of pulsed vortex generator jets over their steady counterpart appears to be the positioning of streamwise vortex much farther into the boundary layer. The circulation and peak vorticity of the primary vortices produced by the pulsed jets, averaged over the pulse duration, are in fact less than those created by the steady jet of the same strength. The larger penetration of the streamwise vortex in the boundary layer is especially evident during the early part of the pulse, which is dominated by the starting vortex ring. Streamwise vortices placed farther into the boundary layer are better capable of entraining and mixing higher momentum flow into the boundary layer. This is the reason for the common practice of specifying solid vortex generators to have vane heights approximately equal to the boundary-layer thickness.

As far as the implementation of pulsed jets is concerned, we propose that only the portion of the pulse associated with the starting vortex ring is beneficial to improving the performance of VGJs. Hence, the injection time of pulsed jets should be long enough to only create the starting vortex ring. Gharib et al.[14] have shown that just the first $4D$ of the injected fluid slug contributes to the circulation of starting vortex ring in free starting jets. Then, the optimal pulse

injection time would be on the order of $4D/V_j$ for a freejet issuing into a quiescent environment. Our estimate, based on the peak core location, produces injection times of the order $6-10D/V_j$. Thus, the optimal pulsed VGJ injection time should be $\tau^* \approx C_1(D/V_j)$, where C_1 is a proportionality constant with a value in the range of 4–8. This argument is solely based on the freejet scaling and our experiments with a single *VR*. Past work has shown that *VR* plays a key role in the jet-in-crossflow dynamics. Therefore, the possibility of *VR* effects on the optimal pulse length in pulsed VGJs should be carefully considered.

If pulsed VGJ are used for separation control on an airfoil, diffuser, or flap of length L, then the timing between successive pulses should be the time it takes the flow to revert to its natural separated state after reattachment by the pulsed jet. This relaxation time scales as C_2L/U_∞, where C_2 is another proportionality constant. Past studies on highly loaded turbine blades have indicated that the relaxation time is on the order of $4L/U_\infty$.[4] Then, with an optimum injection time of $\tau^* \approx C_1(D/V_j)$ one arrives at a minimum duty cycle of $\alpha^* \approx \{1+[C_3(L/D)VR]\}^{-1}$. The proportionality constant of $C_3 = C_2/C_1$ is of order unity. This expression indicates that larger velocity ratios or smaller jet diameters, for a fixed flow rate, would reduce the minimum duty cycle needed for effective separation control. The preceding injection time and duty cycle translate to an optimum pulsing frequency of $f^* = (C_1D/V_j + C_2L/U_\infty)^{-1}$.

If we choose a length scale L equal to the distance from the jet source to the last measurement station in our flat-plate experiments, the preceding estimates produce an injection time of 48 ms and a duty cycle of 0.01. Under these pulsing conditions, a series of starting vortex rings (at the source) would be produced that penetrate to the edge of the boundary layer. With our present setup reproducible pulses could only be generated with injection times of 200 ms or greater. For the 0.25 duty cycle in our study, the injection time was approximately 250 ms, five times larger than the estimated value needed to generate only the starting vortex ring. Further experiments on separated flows are needed to verify the preceding scaling. It is important to reiterate that the preceding arguments are based on the results from a flat-plate boundary layer.

If vortex core placement within the boundary layer can be taken as a direct indicator of the effectiveness of vortex generator jets for separation control, then, at least for the range of our experimental parameters, it appears that pulsing could reduce the VGJ mass flux by a factor of about four from the steady-jet value to get similar or even enhanced benefits. Although the optimum duty cycle just proposed might be quite small for practical applications, other researchers have also found that small duty cycles can be as effective as higher ones with pulsed jets.[4,5] For example, low-pressure turbine blade separation control studies at the U.S. Air Force Research Laboratory have implemented effective pulsed jets with duty cycles as small as 4% (Ref. 4). Solenoid valves with response times of 500 μs are currently available,[1,4] and synthetic jets operate at kilohertz frequencies. Thus, the proposed pulsing conditions would be possible in practical systems.

Conclusions

The streamwise vorticity generated by a pulsed vortex generator jet is compared with that from a steady jet with the same velocity. The jet was pitched 45 deg and skewed 90 deg and had a diameter that was 0.14 times the undisturbed boundary-layer thickness at the jet source. The jet, which had a velocity of $3U_\infty$, was pulsed at a reduced frequency of $f\delta/U_\infty = 0.17$. Two duty cycles of 0.25 and 0.5 were examined. The flowfield was measured at four stations downstream of the jet source, $x/D = 5, 10, 20$, and 30 corresponding to $x/\delta = 0.7, 1.4, 2.8$, and 4.2. Similar to a steady jet, the pulsed jet created a pair of counter-rotating streamwise vortices. One of the vortices was markedly stronger than the other one. For the range of parameters in our study, the following conclusions can be drawn:

1) Phase-averaged data indicate that the maximum circulation and peak vorticity within the pulse are approximately 30% greater than the mean values of the steady jet. On the other hand, the same parameters averaged over the pulse duration are less than those for the steady jet.

2) The maximum circulation and peak vorticity during each pulse decrease exponentially with the distance from the source at a rate comparable to that of the steady jet. The decay of circulation and peak vorticity averaged over the pulse duration is faster than exponential over the range of distances in our study.

3) The primary streamwise vortex generated by the pulsed jet penetrates much farther (~50%) into the boundary layer than the steady jet in both the wall-normal and spanwise directions. The larger penetration takes place during the first portion of the pulse and is caused by the jet starting vortex ring.

The placement of the streamwise vortices farther out in the boundary layer is the essential difference between steady and pulsed jets identified in this study. The strength, as quantified by the average circulation over the pulse duration, of primary vortices generated by pulsed jets is less than the value for a comparable steady jet. The position of the streamwise vortices being farther away from the flow surface can be one of the possible mechanisms for the superior performance of pulsed vortex generator jets observed in the past studies concerning separation control. Other mechanisms, including the unsteady forcing of the vortical structures within separated boundary layers, can also be operative. Detailed flowfield measurements of pulsed vortex generator jets interacting with separated boundary layers are recommended to further elucidate the role of vortex placement in separation control.

Acknowledgments

This work was supported by a GOALI grant from the National Science Foundation (CTS-9631352). The help of D. Bond and K. J. Desabrais with the project is greatly appreciated. Initial discussions with Keith McManus are also acknowledged.

References

[1]McManus, K. R., Legner, H. H., and Davis, S. J., "Pulsed Vortex Generator Jets for Active Control of Flow Separation," AIAA paper 94-2218, June 1994.

[2]McManus, K. R., Joshi, P. B., Legner, H. H., and Davis, S. J., "Active Control of Aerodynamic Stall Using Pulsed Jet Actuators," AIAA Paper 95-2187, June 1995.

[3]McManus, K. R., Ducharme, A., Goldey, C., and Magill, J., "Pulsed Jet Actuators for Suppressing Flow Separation," AIAA Paper 96-0442, Jan. 1996.

[4]Bons, J. P., Sondergaard, R., and Rivir, R. B., "The Fluid Dynamics of LPT Blade Separation Control Using Pulsed Jets," *Proceedings of TURBOEXPO 2001: International Gas Turbine Conference*, American Society of Mechanical Engineers, Paper 2001-GT-0190, 2001.

[5]Magill, J. C., and McManus, K. R., "Exploring the Feasibility of Pulsed Jet Separation Control for Aircraft Configurations," *Journal of Aircraft*, Vol. 38, No. 1, 2001, pp. 48–56.

[6]Johari, H., Zhang, Q., Rose, M., and Bourque, S., "Impulsively Started Turbulent Jets," *AIAA Journal*, Vol. 35, No. 4, 1997, pp. 657–662.

[7]Bremhorst, K., and Hollis, P. G., "Velocity Field of an Axisymmetric Pulsed, Subsonic Air Jet," *AIAA Journal*, Vol. 28, No. 12, 1990, pp. 2043–2049.

[8]Crow, S. C., and Champagne, F. H., "Orderly Structure in Jet Turbulence," *Journal of Fluid Mechanics*, Vol. 48, Pt. 3, 1971, pp. 547–591.

[9]Johari, H., Pacheco-Tougas, M., and Hermanson, J. C., "Penetration and Mixing of Fully-Modulated Turbulent Jets in Crossflow," *AIAA Journal*, Vol. 37, No. 7, 1999, pp. 842–850.

[10]Eroglu, A., and Breidenthal, R. E., "Structure, Penetration, and Mixing of Pulsed Jets in Crossflow," *AIAA Journal*, Vol. 39, No. 3, 2001, pp. 417–423.

[11]Johari, H., and McManus, K. R., "Visualization of Pulsed Vortex Generator Jets for Active Control of Boundary Layer Separation," AIAA Paper 97-2021, June 1997.

[12]Compton, D. A., and Johnston, J. P., "Streamwise Vortex Production by Pitched and Skewed Jets in a Turbulent Boundary Layer," *AIAA Journal*, Vol. 30, No. 3, 1992, pp. 640–647.

[13]Rixon, G. S., "The Interaction of Vortex Generator Jets with a Turbulent Boundary Layer," M. S. Thesis, Dept. of Mechanical Engineering, Worcester Polytechnic Inst., Worcester, MA, Aug. 2000; also *Journal of Fluids Engineering* (to be published).

[14]Gharib, M., Rambod, E., and Shariff, K., "A Universal Time Scale for Vortex Ring Formation," *Journal of Fluid Mechanics*, Vol. 360, 1998, pp. 121–140.

A. R. Karagozian
Associate Editor